

Catalytic Pathway of Serine Proteases: Classical and Quantum Mechanical Calculations

Valerie Daggett,[†] Stefan Schröder,[‡] and Peter Kollman*

Contribution from the Department of Pharmaceutical Chemistry, University of California at San Francisco, San Francisco, California 94143-0446. Received December 27, 1990

Abstract: Herein we describe semiempirical molecular orbital calculations of serine protease catalyzed hydrolysis of amides and esters. We found that attack of the substrate by the active site serine to form the tetrahedral intermediate was the rate-limiting step with both substrates. The lowest energy path for formation of the tetrahedral intermediate was for Ser to approach the substrate, followed by coupled heavy atom movement and proton transfer to complete the reaction. The effect of the environment on catalysis was estimated by calculating molecular mechanical interaction energies in both a noncovalent trypsin-peptide complex and a model for the transition state in which a covalent bond is imposed between O_γ of the serine and the carbonyl carbon of the substrate. We found that the environment itself was important in stabilizing the transition state compared to the Michaelis complex in addition to stabilization by the aspartic acid of the catalytic triad and the oxyanion hole. A molecular dynamics simulation was also performed of the noncovalent complex to test the importance of motion in the active site in the early stages of catalysis.

Introduction

One of the biggest challenges in biochemistry is to understand the molecular basis of enzyme catalysis. The serine protease family of endopeptidases provides one of the best systems for addressing this question. There is more direct evidence about the mechanism of catalysis and structures of intermediates in the reaction of serine proteases than any other enzyme or enzyme family.¹ Serine proteases have also been the subject of numerous theoretical studies.

All serine proteases contain the catalytic triad—Asp—His—Ser.² The purpose of this arrangement of residues in the active site is presumably to make the serine sufficiently nucleophilic that it attacks the carbonyl carbon of the amide or ester substrate (Figure 1), thus beginning the catalytic process. Serine's attack on the substrate results in formation of a tetrahedral intermediate (TET₁, Figure 1), which breaks down to yield the acylenzyme intermediate, EA. The second part of the reaction begins at this point with hydrolysis of the acylenzyme intermediate, resulting in formation of the second tetrahedral intermediate, TET₂. Collapse of this intermediate yields the enzyme-product complex. All serine proteases also contain an oxyanion hole, which is generally made up of two backbone amide hydrogens.² The main purposes of the oxyanion hole are to stabilize the oxyanion of the tetrahedral intermediates and to stabilize the developing negative charge en route to the tetrahedral conformation.

Some theoretical studies indicate³ or assume⁴ that the proton is transferred from the serine to the histidine prior to attack of the substrate, such that the transferred proton is not a direct participant in the bond making and breaking events occurring in the transition state. This sequence of steps is inconsistent with the experimental kinetic isotope effects that suggest that there is protonic bridging in the transition state.⁵ Many of these theoretical studies also support the double-proton-transfer mechanism, whereby the Asp abstracts a proton from the histidine following transfer from the serine.⁶⁻⁸ This mechanism was first suggested to be wrong on the basis of theoretical studies by Hayes and Kollman.⁹ Although their results were not definitive in ruling out the double-proton-transfer mechanism, they certainly were strongly suggestive that a single proton transfer was favored. Some experimental evidence has been interpreted to rule out the double-proton-transfer mechanism,¹⁰⁻¹² although not all researchers in the field agree.⁵ Most of the theoretical studies of serine protease catalysis have only dealt with the first part of the reaction pathway—acylation (Figure 1).⁴ In addition, many of the previous

studies used severely truncated forms of the catalytic triad¹³ or have completely left portions out, such as the histidine.⁶ For these reasons, we decided to explore the entire serine protease catalyzed pathway in detail with the functional forms of the catalytic triad residues present.

This paper presents the results of semiempirical molecular orbital calculations of serine protease catalyzed hydrolysis of amides and esters. First, control calculations were performed of model compounds relevant to the reaction, and these are presented in the accompanying paper. Initially, we employed two molecular models, AM1¹⁴ and PM3.¹⁵ We found AM1 to be unsatisfactory for the model compounds. For this reason, the calculations described here were performed with PM3. The calculations of the reaction pathway included slightly truncated versions of the residues making up the catalytic triad extracted from the trypsin X-ray crystal structure (Figure 2). The oxyanion hole was represented by two water molecules in the positions of the main chain groups making up the oxyanion hole in the crystal structure. Acylation was investigated using both amide and ester substrates.

We found that formation of the first tetrahedral intermediate was the rate-limiting step in the reaction pathway with both substrates (Figure 3). The lowest energy path for formation of the tetrahedral intermediate was for serine to approach the substrate, followed by coupled heavy atom movement and proton transfer to complete the reaction; we believe our description of this sequence of events to be novel. When one considers the effect of fluctuations in the enzyme on the process, deacylation becomes

(1) Fersht, A. R. *Enzyme Structure and Mechanism*; W. H. Freeman & Co.: New York, 1985.

(2) Kraut, J. *Annu. Rev. Biochem.* **1977**, *46*, 331-358.

(3) Scheiner, S.; Lipscomb, W. *Proc. Natl. Acad. Sci. U.S.A.* **1976**, *73*, 432.

(4) Warshel, A.; Russell, S. *J. Am. Chem. Soc.* **1986**, *108*, 6569-6579.

(5) Schowen, R. L. *Molecular Structure and Energetics*. In *Principles of Enzyme Activity*; Liebman, J. F., Greenberg, A., Eds.; VCH Publishers: Weinheim, FRG, 1988; Vol. 9.

(6) Dewar, M. J. S.; Storch, D. M. *Proc. Natl. Acad. Sci. U.S.A.* **1985**, *82*, 2225-2229.

(7) Scheiner, S.; Kleier, D. A.; Lipscomb, W. N. *Proc. Natl. Acad. Sci. U.S.A.* **1975**, *72*, 2606.

(8) Umeyama, H.; Imamura, A.; Nagato, C.; Hanano, M. *J. Theor. Biol.* **1973**, *41*, 485.

(9) Hayes, D. M.; Kollman, P. A. In *Catalysis in Chemistry and Biochemistry: Theory and Experiment*; Pullman, B., Ed.; D. Reidel Publishing Co.: Boston, MA, 1979.

(10) Kossiakoff, A. A.; Spencer, S. A. *Biochemistry* **1981**, *20*, 6462-6474.

(11) Bachovchin, W. W. *Biochemistry* **1986**, *25*, 7751.

(12) Steitz, T. A.; Shulman, R. G. *Annu. Rev. Biophys. Bioeng.* **1982**, *11*, 419.

(13) Stamato, F. M. L. G.; Tapia, O. *Int. J. Quantum Chem.* **1988**, *33*, 187-194.

(14) Dewar, M. J. S.; Zoebisch, E. G.; Healy, E. F.; Stewart, J. J. P. *J. Am. Chem. Soc.* **1985**, *107*, 3902.

(15) Stewart, J. J. P. *J. Comput. Chem.* **1989**, *10*, 209-220.

[†]Current address: Beckman Laboratories for Structural Biology, Department of Cell Biology, Stanford University Medical School, Stanford, CA 94305-5400.

[‡]Current address: Schering AG, PCH/TCH, D-1000 Berlin 65, Germany.

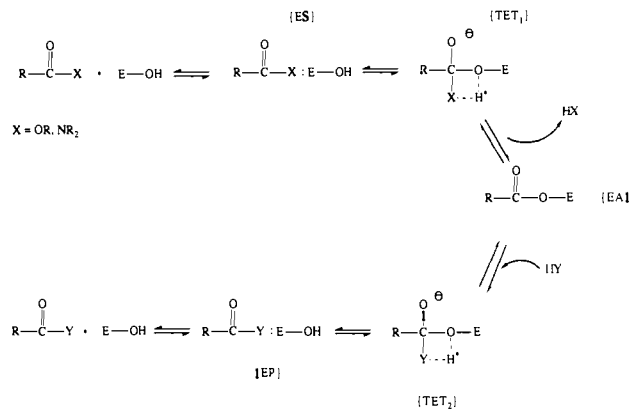


Figure 1. Schematic representation of the reaction pathway of serine protease catalysis of amide and ester bonds. E-OH represents the enzyme's hydroxyl group on Ser 177. The following abbreviations are used: ES denotes the Michaelis complex; TET₁ represents the first tetrahedral intermediate; EA represents the acylzyme intermediate; HY represents a water molecule in our scheme; TET₂ is the second tetrahedral intermediate following water attack of the acylzyme intermediate; and EP denotes the enzyme-product complex.

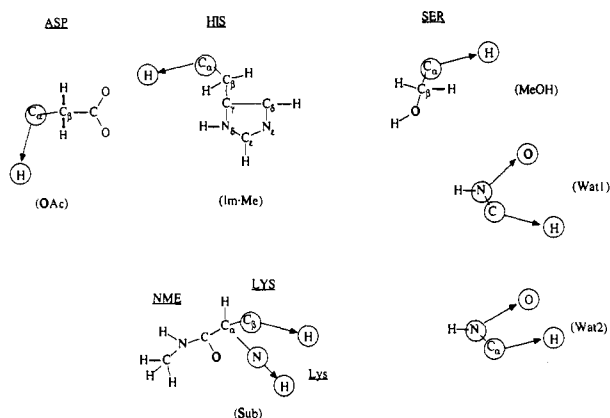


Figure 2. Key active site residues in serine proteases. The atom changes illustrated here are for adapting the residues from the refined crystal structure of trypsin to the reduced representation (names in parenthesis) for the quantum mechanical calculations. See text for details.

the rate-limiting step in ester hydrolysis. The importance of different active site residues and the environment in stabilizing the substrate was addressed by evaluating particular interactions in full, solvated enzyme-substrate models. These interaction energies were calculated for both a noncovalent enzyme-substrate complex and a model for the tetrahedral intermediate in which a covalent bond was formed between the serine and substrate. The oxyanion hole and Asp greatly stabilized the active site region of the tetrahedral intermediate, and presumably the transition-state structure. The environment itself, excluding the active site residues and the oxyanion hole, was important in stabilizing the scissile bond of the substrate in the tetrahedral intermediate versus the Michaelis complex. A molecular dynamics simulation was also performed of the noncovalent complex to investigate possible roles of motion in catalysis. Our results are discussed in light of the available experimental data.

Methods

Preparation of the Molecular Mechanical Serine Protease Model. We used the bovine trypsin crystal structure of Chambers and Stroud (3ptp, 1.5-Å resolution).¹⁶ We added the substrate Ace-Phe-Val-Lys-Nme using the computer graphics package MIDAS.¹⁷ This tripeptide was used because it is catalytically very efficient¹⁸ and because it was used in an

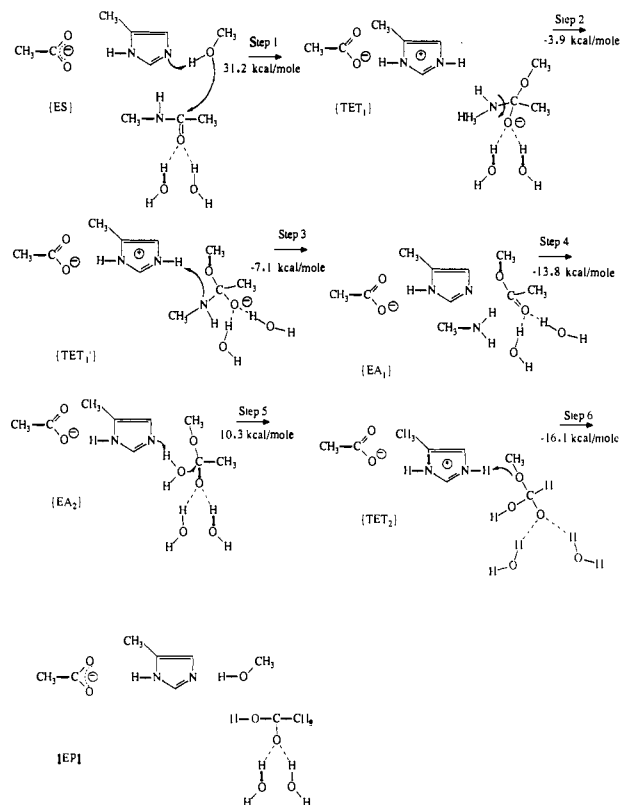


Figure 3. Steps along the reaction pathway of serine protease catalyzed peptide bond cleavage. The differences in energy given for each step are between energies for the fully optimized systems.

earlier study from this research group.¹⁹ Polar and steric interactions were considered in aligning the substrate in the binding pocket. Counterions were positioned near free charged surface residues of the protein (thirteen chloride ions and three sodium ions). In addition to the counterions, the model contained the internal calcium ion identified in the crystal structure. The overall charge of the system was -1.

It was necessary to refine the coordinates prior to extracting the catalytically important residues for the quantum mechanical calculations. The molecular mechanics program AMBER version 3.0 was used for the calculations described below.²⁰ Standard all-atom parameters were used for the catalytically important residues (His 40, Asp 84, Ser 177, and the capped, amidated Lys of the substrate).²¹ Standard united atom parameters were used for all other residues.²² The energy of the system was minimized to a root-mean-square (rms) energy gradient of 0.1 kcal/(mol Å²) to remove bad contacts. Then, a sphere of TIP3P water molecules²³ extending 20 Å in any direction from the hydroxyl oxygen of Ser 177 was generated; this resulted in the introduction of 384 water molecules. Following the addition of the water molecules, the energy of the system was minimized. For this minimization, only those residues within 15 Å of Ser 177 were allowed to move. A 12-Å nonbonded cutoff was used. Minimization was carried out using the steepest descent method for 200 steps, followed by conjugate gradient minimization to a rms energy gradient of 0.1 kcal/(mol Å²). The resulting structure was used as the starting structure for the semiempirical calculations, for molecular dynamics simulations, and for forming a model of the tetrahedral intermediate.

Construction of the Quantum Mechanical Active Site Model. After the trypsin model was refined, the Cartesian coordinates for His 40, Asp 84, Gly 175, Ser 177, and N-methylated Lys of the substrate were extracted from the rest of the system for the quantum mechanical calculations. Abbreviated forms of these residues were used (Figure 2). To make the

(19) Weiner, S. J.; Seibel, G. L.; Kollman, P. A. *Proc. Natl. Acad. Sci. U.S.A.* **1986**, *83*, 649-653.

(20) Singh, U. C.; Weiner, P. K.; Caldwell, J.; Kollman, P. A. *AMBER 3.0*; University of California: San Francisco, 1986.

(21) Weiner, S. J.; Kollman, P. A.; Nguyen, D. T.; Case, D. A. *J. Comput. Chem.* **1986**, *7*, 230.

(22) Weiner, S. J.; Kollman, P. A.; Case, D. A.; Singh, U. C.; Ghio, C.; Alagona, G.; Profeta S., Jr.; Weiner, P. *J. Am. Chem. Soc.* **1984**, *106*, 765-784.

(23) Jorgensen, W. L.; Chandrasekhar, J.; Madura, J.; Impey, R. W.; Klein, M. L. *J. Chem. Phys.* **1983**, *79*, 926-935.

(16) Chambers, J.; Stroud, R. *Acta Crystallogr.* **1977**, *B33*, 1824-1833.
(17) Jarvis, L.; Huang, C.; Ferrin, T.; Langridge, R. *UCSF MIDAS*; University of California: San Francisco, 1985.

(18) Pozsgay, M.; Szabo, G.; Bajusz, S.; Simonsson, R.; Caspar, R.; Elodi, P. *Eur. J. Biochem.* **1981**, *115*, 497-502.

conversion to the truncated residues, some of the initial hydrogen positions were taken from the coordinates of the appropriate carbon or nitrogen, thus terminating the chain (the circled atoms in Figure 2 were replaced by hydrogens or oxygens). Instead of including the main chain atoms that make up the oxyanion hole (residues 175 and 177), we positioned two water molecules in their positions to decrease the size of the system.

The calculations reported below were carried out using the PM3¹⁵ molecular model as implemented within a modified version of the MOPAC 5.0 program.²⁴ All of the reactions were followed by using the reaction coordinate method²⁵ with an internuclear distance or dihedral angle specified as the reaction coordinate. The active site model described above, and shown schematically in Figure 2, contained a number of long bonds because of the atom type swaps made to truncate the system. Therefore, the positions of the swapped atoms were optimized by minimizing their energy while "freezing" the geometry of all other groups (i.e., by turning off the optimization flag). To further refine the model prior to reaction coordinate calculations, the distance between the hydroxyl oxygen of the Ser 177 mimic (MeOH) and the carbonyl carbon of the substrate was optimized while all other parameters were fixed. Then, the entire system was optimized followed by further high-precision optimization (i.e., by use of the PRECISE flag). The resulting geometries (ES of Figure 3) were used for the model calculations described in the previous paper and in the reaction coordinate studies described below.

Semiempirical Empirical Reaction Coordinate Calculations. To simulate the reaction shown schematically in Figure 3, slightly different procedures were used for the different steps. For the first step, the reaction coordinate method²⁵ was used with the proton-transfer distance between the hydroxyl hydrogen of the Ser mimic to the free nitrogen of the His model specified as the reaction coordinate (decreasing from 1.77 to 1.00 Å). Full geometry optimization was accomplished at each point along the reaction path, with the exception of the distance between the hydroxyl oxygen of the Ser and the carbonyl carbon of the substrate which was frozen (not optimized) at four different distances (3.3, 2.7, 2.1, and 1.5 Å). So, the proton-transfer reaction was carried out at each of the C–O distances. The grid search approach was used to address both the proton-transfer step and serine's attack on the substrate to avoid forcing the order of the steps.

The second step of the reaction in Figure 3 with the amide substrate involved rotation about the scissile bond. This step was accomplished by using the appropriate dihedral angle (carbon of the methyl group on N, N, C, carbonyl oxygen) as the reaction coordinate and rotating the angle from 40° to 0° and finally to –40°. Step 3 involved formation of the acylenzyme intermediate. The distance between the nitrogen of the substrate and the hydrogen on N_i of the His was the reaction coordinate, decreasing from 2.67 to 1.85 to 1.00 Å. During the proton transfer, cleavage of the C–N bond (or C–O with the ester) of the substrate occurred, leaving the free amine and the acylenzyme intermediate.

The next step in the reaction was to replace the amine or alcohol by a water molecule (step 4). The water molecule was superimposed on the NH₂ portion of the methylamine group or the hydroxyl group of the methanol to get its initial position, followed by full geometry optimization. Step 5 represents attack of water on the acylenzyme, leading to formation of the second tetrahedral intermediate. The grid search approach was used as described in step 1. In this case, the distances between the water's oxygen and the carbonyl carbon were fixed at 3.13, 2.30, and 1.50 Å. At these fixed positions, the distance between N_i and one of the water's hydrogens was decreased from 1.77 to 1.40 Å. The final step, regeneration of the enzyme with bound product, was accomplished by transferring the proton from N_i of the His mimic to the methoxy group representing the serine (the distance began at 1.81 and was decreased to 1.40 and then 1.00 Å, step 6). The bond between the serine and the product broke as a result of the transfer. All of the final structures resulting from the reactions described above were fully optimized with respect to all degrees of freedom. To determine the importance of the Asp and the oxyanion hole in stabilizing the intermediates along the reaction pathway, the energy of the optimized structures was reevaluated, leaving out the Asp mimic and the two water molecules representing the oxyanion hole.

Molecular Mechanics and Dynamics Calculations. To further estimate the role of the environment in stabilizing the substrate both in the non-covalent enzyme–substrate complex and in the tetrahedral intermediate, we evaluated various interactions in the full system using AMBER.²⁰ Interactions were evaluated in the minimized enzyme–substrate complex described above. The tetrahedral intermediate model was constructed from the minimized structure by imposing a covalent bond between O_γ

of the serine and the carbonyl carbon of the substrate. In this complex, the His was positively charged, some nonstandard internal parameters were used, and the charges of the peptide bond atoms were altered to give an oxyanion.²⁶ The charges were derived for the structure of the first tetrahedral intermediate from the quantum mechanical studies with the amide substrate. Point charges needed to reproduce the semiempirical quantum mechanical potential (using PM3) around the CH₃–NMA complex described in the previous paper were calculated using the approach described by Besler et al.²⁷ The equilibrium values for the distance, angle, and torsional parameters of the force field were taken from the fully optimized tetrahedral structure, and the force constants used were for like groups from the standard parameter list.²² The energies reported were calculated using the potential function in ref 22, except that a sigmoidal distance-dependent dielectric function was used,²⁸ instead of $\epsilon = 1$ or $\epsilon = r$, to screen the long-range electrostatic interactions more effectively.

A 50-ps molecular dynamics simulation of the noncovalent trypsin–peptide complex was also performed. The temperature was maintained at 300 K by coupling to an external heating bath.²⁹ An 8-Å nonbonded cutoff was employed with the nonbonded list updated every 50 steps. A linear distance-dependent dielectric function was used ($\epsilon = r$) even though water molecules were present (e.g., given the small number of water molecules included, the full dielectric effect of the solvent will not be present; instead a macroscopic dielectric constant is warranted). The SHAKE algorithm³⁰ was employed so that 0.002 ps time steps could be used. Only those residues within 12 Å of the O_γ of Ser 177 were allowed to move. Structures were saved every 0.2 ps, resulting in 250 structures for analysis.

Results

We have performed semiempirical molecular orbital calculations of serine protease catalyzed amide and ester hydrolysis. We also present molecular mechanical results aimed at estimating the importance of different groups in stabilizing the tetrahedral intermediate relative to the Michaelis complex and the importance of dynamical fluctuations in the Michaelis complex.

Semiempirical Quantum Mechanical Calculations. Reaction Pathway. We calculated the steps along the reaction pathway shown in Figure 3, with the amide substrate shown. The starting structure (ES) was extracted from the active site of minimized trypsin and then optimized using the PM3 model. The relative orientations of the active site residues were fairly well maintained in the truncated system (compare MIN and ES in Table I), which was the starting structure for the calculations along the reaction pathway. The reaction coordinate method was used for the steps along the pathway, where the reaction coordinate for each step is specified in Figure 3 by an arrow. The energy differences given in the figure are between the energies of the optimized structures and also represent activation energies except where noted below.

The first step in the serine protease pathway represents proton transfer from the serine to the histidine and attack of the carbonyl carbon by the serine to form the tetrahedral intermediate. Since there were two reaction coordinates for this first step, we used a grid approach, with proton transfer (d_1 of Tables II and III) occurring at fixed, but different, distances between the serine oxygen and the carbonyl carbon (d_2 of Tables II and III). This type of approach allowed us to investigate the energetics of different possible modes of forming the tetrahedral intermediates. The lowest energy path is shown in italics in both tables. The most favorable path for both substrates was for approach of the

(26) The atom type changed for O_γ of the Ser in the tetrahedral intermediate to OS, and the carbonyl carbon of the substrate Lys (e.g., the atom being attacked by O_γ during catalysis) became CT; atom types and parameters are explained in refs 21 and 22. The following parameters were added to the standard list: bond, CT–O, $K_r = 320$ kcal/(mol Å), $R_{eq} = 1.30$ Å; CT–OS, 800 kcal/(mol Å), 1.50 Å; angle, CT–CT–O, $K_\theta = 80$ kcal/(mol rad²), $\theta_{eq} = 84.1^\circ$; N–CT–O, 80, 112.7 (same order and same units as previous value); HC–CT–OS, 80, 109.5; OS–CT–O, 400, 109.5; OS–CT–N, 400, 109.5; CT–OS–CT, 400, 109.5; OS–CT–CT, 400, 109.5; OS–CT–H, 400, 109.5. The r_{eq} and θ_{eq} values are those observed in the quantum mechanical model of the tetrahedral intermediate.

(27) Besler, B. H.; Merz, K. M., Jr.; Kollman, P. A. *J. Comput. Chem.* **1990**, *11*, 431.

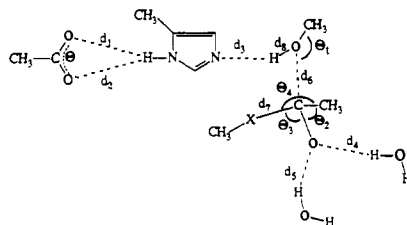
(28) Daggett, V.; Kollman, P. A.; Kuntz, I. D. *Biopolymers* **1991**, *31*, 285.

(29) Berendsen, H. J. C.; Postma, J. P. M.; van Gunsteren, W. F.; DiNola, A.; Haak, J. R. *J. Chem. Phys.* **1984**, *81*, 3684.

(30) Ryckaert, J.; Ciccoliti, G.; Berendsen, H. J. C. *J. Comput. Phys.* **1977**, *23*, 327.

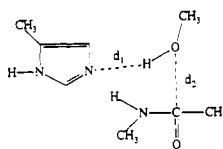
(24) Merz, K. M., Jr.; Besler, B. H. QCPE Program No. 589. *QCPE Bull.* **1990**, *10*, 15.

(25) Dewar, M. J. S.; Kirschner, S. J. *J. Am. Chem. Soc.* **1971**, *93*, 4290.

Table I. Distances between Active Site Residues in AMBER-Minimized Trypsin (MIN) and between Corresponding Optimized Model Structures in the Acylation Path^a

property	amide substrate (X = NH)					ester substrate (X = O)			
	MIN	ES	TET ₁	TET ₁ '	EA ₁	ES	TET ₁	EA ₁	
<i>d</i> ₁	1.76	1.70	1.65	1.66	1.69	1.70	1.65	1.71	
<i>d</i> ₂	2.15	2.15	2.42	2.44	2.49	2.52	2.43	2.57	
<i>d</i> ₃	1.96	1.76	1.00	1.02	1.76	1.77	1.02	1.79	
<i>d</i> ₄	1.84	1.81	1.77	1.75	1.80	1.82	1.75	1.81	
<i>d</i> ₅	1.90	2.53	1.75	1.74	1.77	2.55	2.45	2.63	
<i>d</i> ₆	2.91	3.30	1.50	1.48	1.41	3.32	1.48	1.36	
<i>d</i> ₇	1.34	1.42	1.53	1.54	1.78	1.36	1.44	5.55	
<i>d</i> ₈	0.97	0.98	1.75	1.75	1.54	0.98	1.74	5.83	
<i>θ</i> ₁	104	154	118	118	119	153	117	120	
<i>θ</i> ₂	121	123	116	116	120	127	117	128	
<i>θ</i> ₃	122	120	113	112		120	116		
<i>θ</i> ₄	116	117	108	111		114	107		
ΔH_f		-357.81	-326.63	-330.53	-337.64	-396.19	-374.63	-397.78	

^a See Figure 3 for explanation of abbreviations. Distances are in angstroms, angles are in degrees, and the heat of formation is in kilocalories per mole.

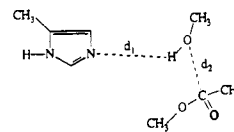
Table II. Energies along the Reaction Pathway for Formation of the First Tetrahedral Intermediate with an Amide Substrate (kcal/mol)^a

fixed <i>d</i> ₂ (Å)	<i>d</i> ₁ (Å)		
	1.77	1.40	1.00
3.30	-357.8	-345.4	-331.3
2.70	-355.5	-343.5	-328.6
2.10	-344.1	-333.2	-322.8
1.50	-315.0	-310.8	-326.3

^a The calculations included, in addition to the compounds shown, the Asp and oxyanion hole mimics as shown in step 1 of Figure 3. The low-energy path is italic.

serine, while the Ser...His hydrogen bond was maintained. When the O-C bond distance was 2.10 Å, partial transfer of the proton was favored, and from that point simultaneous transfer of the proton and formation of the C-O bond gave the low-energy path. This progression yielded an activation energy of 31.5 kcal/mol for the amide and 22.3 kcal/mol with the ester. A slight approach of Ser to the substrate (3.3 → 2.7 Å), followed by concerted attack and proton transfer (moving along the diagonal in Tables II and III), gave the same activation energy in both cases. When these two reaction coordinates were considered separately, complete proton transfer followed by methoxide attack on the substrate, the calculated activation energies were 35.0 and 31.5 kcal/mol for the amide and ester, respectively.

Step 1 yielded the tetrahedral intermediate for acylation (TET₁, optimized structure shown in Figure 4). As can be seen, the substrate carbon did indeed become tetrahedral (compare structures ES and TET₁ of Figure 4). In amide hydrolysis, the hydrogen bonds to the water molecules making up the oxyanion hole improved in forming the oxyanion, while other interactions remained roughly the same (Table I). The hydrogen bonds to the oxyanion hole did not improve upon forming the tetrahedral intermediate with the ester substrate, however (Table I). An isomer of TET₁ was then constructed by passing a proton from the positively charged His to the Asp. This process had an ac-

Table III. Energies along the Reaction Pathway for Formation of the First Tetrahedral Intermediate with an Ester Substrate (kcal/mol)^a

fixed <i>d</i> ₂ (Å)	<i>d</i> ₁ (Å)		
	1.77	1.40	1.00
3.30	-396.3	-384.9	-369.5
2.70	-394.7	-382.8	-367.6
2.10	-382.0	-374.0	-364.8
1.50	-360.6	-357.3	-374.2

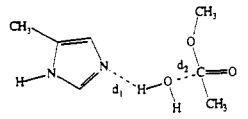
^a The calculations included, in addition to the compounds shown, the Asp and oxyanion hole mimics as shown in step 1 of Figure 3. The low-energy path is italic.

tivation energy of 3.9 kcal/mol. The energy of the resulting optimized structure was 15.7 kcal/mol more stable than TET₁ (-342.31 vs -326.63 kcal/mol). Hence, the triple ion is a local minimum, with the double-proton-transferred structure more stable in isolation in vacuo.

The next step in the reaction pathway for the amide substrate involved rotation about the substrate's nitrogen. This process was favorable, by -3.9 kcal/mol, and without a barrier to rotation. Rotation of this bond left the nitrogen of the substrate in a better position to abstract the proton on the histidine (3.10 Å in TET₁ versus 2.84 Å in TET₁'). All other interactions shown in Table I were maintained.

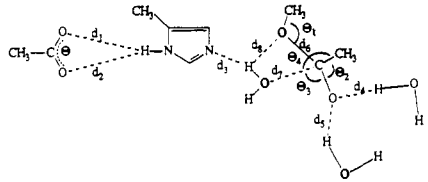
The next step in the pathway involved transfer of a proton from the positively charged histidine to the nitrogen of the substrate. As a result of this proton transfer the C-N bond of the amide or C-O bond of the ester was cleaved, leaving the acylenzyme intermediate (EA₁) and methylamine or methanol. This process was favorable and again without an activation barrier. After cleavage, the histidine remained hydrogen bonded to the methylamine or methanol (Table I). Step 4 of Figure 3 represents not a chemical step but instead the exchange of methylamine or methanol for water (EA₂).

After positioning the water molecule, there was a proton transfer from the water to the histidine and attack of the carbonyl carbon

Table IV. Energies along the Reaction Pathway for Formation of the Second Tetrahedral Intermediate (kcal/mol)^a


fixed d_2 (Å)	d_1 (Å)		
	1.77	1.40	1.00
3.13	-396.7	-384.4	-357.5
2.30	-393.2	-387.1	-359.3
1.50	-379.1	-375.8	-384.9

^aThe calculations included, in addition to the compounds shown, the Asp and oxyanion hole mimics as shown in step 5 of Figure 3. The low-energy path is italic.

Table V. Distances between Active Site Residues in AMBER-Minimized Trypsin (MIN) and between Corresponding Optimized Model Structures in the Deacylation Path^a


property	MIN	EA ₂	TET ₂	EP
d_1	1.76	1.71	1.66	1.70
d_2	2.15	2.52	2.39	2.51
d_3	1.96	1.78	1.05	1.76
d_4	1.84	1.84	1.77	1.83
d_5	1.90	1.81	1.75	1.82
d_6	2.91	1.35	1.46	3.66
d_7	1.34	3.90	1.42	1.34
d_8	0.97	3.80	1.81	0.98
θ_1	104	121	117	128
θ_2	121	127	119	127
θ_3	122		104	117
θ_4	116		113	116
ΔH_f		-351.44	-341.14	-337.24

^aSee Figure 3 for explanation of abbreviations. Distances are in angstroms, angles are in degrees, and the heat of formation is in kilocalories per mole.

of the acylated serine by water, yielding the second tetrahedral intermediate, TET₂ (step 5, Figure 3). Here again we used a grid approach to examine the energetics of different possible pathways for this process (Table IV). The lowest energy pathway is in italics in Table IV and had an activation energy of 15.6 kcal/mol. The concerted process with simultaneous proton transfer and attack also had an activation energy of 15.6 kcal/mol (moving along the diagonal in Table IV). The other possible path had a much higher activation energy. To first transfer the proton to give attack by a hydroxyl group yielded a 39.1 kcal/mol barrier, which was due entirely to abstracting the proton (Table IV). This second tetrahedral intermediate (TET₂) was very similar to the first tetrahedral intermediate (TET₁) (Figure 4 and Tables I and V).

The final step in this process was transfer of a proton from the histidine to the serine and regeneration of the resting state of the active site residues with bound product (EP in Figure 4). Breakdown to product occurred as result of this proton transfer. The hydrogen bonds to the oxyanion hole became slightly longer with loss of the oxyanion (structures TET₂ and EP of Figure 4 and Table V). Although this appeared to be a favorable process, this step had an activation barrier of 14.2 kcal/mol.

Effect of Active Site Asp and Oxyanion Hole. After investigating the serine protease pathway with the residues of the catalytic triad and oxyanion hole mimics, we examined the importance of the Asp and the oxyanion hole to this reaction with the amide substrate. To this end, we took the optimized structures (Figure 4) along the pathway and evaluated their energies without the

Table VI. Molecular Mechanical Interaction Energies (kcal/mol) in a Trypsin-Triptide Michaelis Complex and in a Model for the Tetrahedral Intermediate

interaction ^a	KM	TET
His 40, Asp 84, HN of Gly 175, Ser 177, and scissile bond with system	-94.3	-120.2
scissile bond with system	-12.5	-24.6
scissile bond with HN of Gly 175	-1.0	-15.3
scissile bond with HN of Ser 177	-0.3	-13.2
scissile bond with His 40	-1.0	-8.7
scissile bond with Asp 84	0.0	1.0
scissile bond with Ser 177	-4.2	2.1

^aScissile bond is composed of the main chain atoms of the substrate: HN and N of residue Nme and carbonyl group of Lys. System is all other residues of the substrate, the protein, and the water molecules.

groups in question. The results are shown schematically in Figure 5, with the values for the reaction with the ester given for comparison. As can be seen, removing the Asp mimic and oxyanion hole waters drastically destabilized the three tetrahedral intermediates along the pathway (structures TET₁, TET₁', and TET₂ of Figure 5). In each of these cases, the Asp contributed more to stabilization of the tetrahedral species than did the water molecules representing the oxyanion hole. These groups were not as important in the stabilization of the other structures, except for approximately 6 kcal/mol stabilization of the acylzyme intermediate provided by the oxyanion hole (EA₁). Asp was actually destabilizing for the acylzyme intermediates and the enzyme-product complex (structures EA₁, EA₂, and EP).

Classical Calculations. Molecular Mechanical Interaction Energies. Table VI gives molecular mechanical interaction energies between different groups in the noncovalent and covalent enzyme-substrate complex. The first entry represents the interaction of the catalytic triad, the oxyanion hole, and the scissile bond of the substrate (NHCO) with the environment (all other protein, substrate, and water atoms). This interaction is more favorable in the tetrahedral complex than in the Michaelis complex by approximately 26 kcal/mol. This indicates that the environment itself is important in stabilizing the tetrahedral intermediate, in addition to the interactions with the oxyanion hole and catalytic triad residues. The difference between the two states was not due to significant structural changes in the protein; the changes were localized to the immediate active site region. The root-mean-square deviation in the backbone atoms (N, C α , C) between the two structures was 0.04 Å, with a maximum deviation of 0.44 Å of the α carbon of Ser 177.

Some of the interactions between the scissile bond and other active site residues are also presented in Table VI. Interactions between the peptide bond and the oxyanion hole (HN of Gly 175 and HN of Ser 177) improved dramatically in going from the noncovalent to covalent complex. Interactions with His 40 were also better in the tetrahedral complex, by 8 kcal/mol. The interaction between Ser 177 and the peptide bond it attacks was favorable in the noncovalent complex, thereby aiding catalysis.

Molecular Dynamics Simulation. A molecular dynamics simulation was also performed of the noncovalent trypsin-substrate complex to address the possible role of motion in the early stages of catalysis. The distance between O γ of the serine and the carbonyl carbon of the scissile bond was 2.9 Å on average during the 50-ps trajectory. The minimum distance observed during the simulation was 2.5 Å. The hydrogen bond distance between His 40 and Ser 177 was an average of 2.5 Å during the simulation. This hydrogen bond was broken 24% of the simulation time (the two atoms were considered to be involved in a hydrogen bond if the distance was less than 3 Å). But, even though the hydrogen bond was broken a good deal of the time, it was only broken for 0.4 ps on average.

Discussion

The accompanying paper describes calculations of model compounds for the serine protease catalyzed hydrolysis pathway using the AM1 and PM3 molecular models. From that study, we found PM3 to be the most appropriate model to use for the

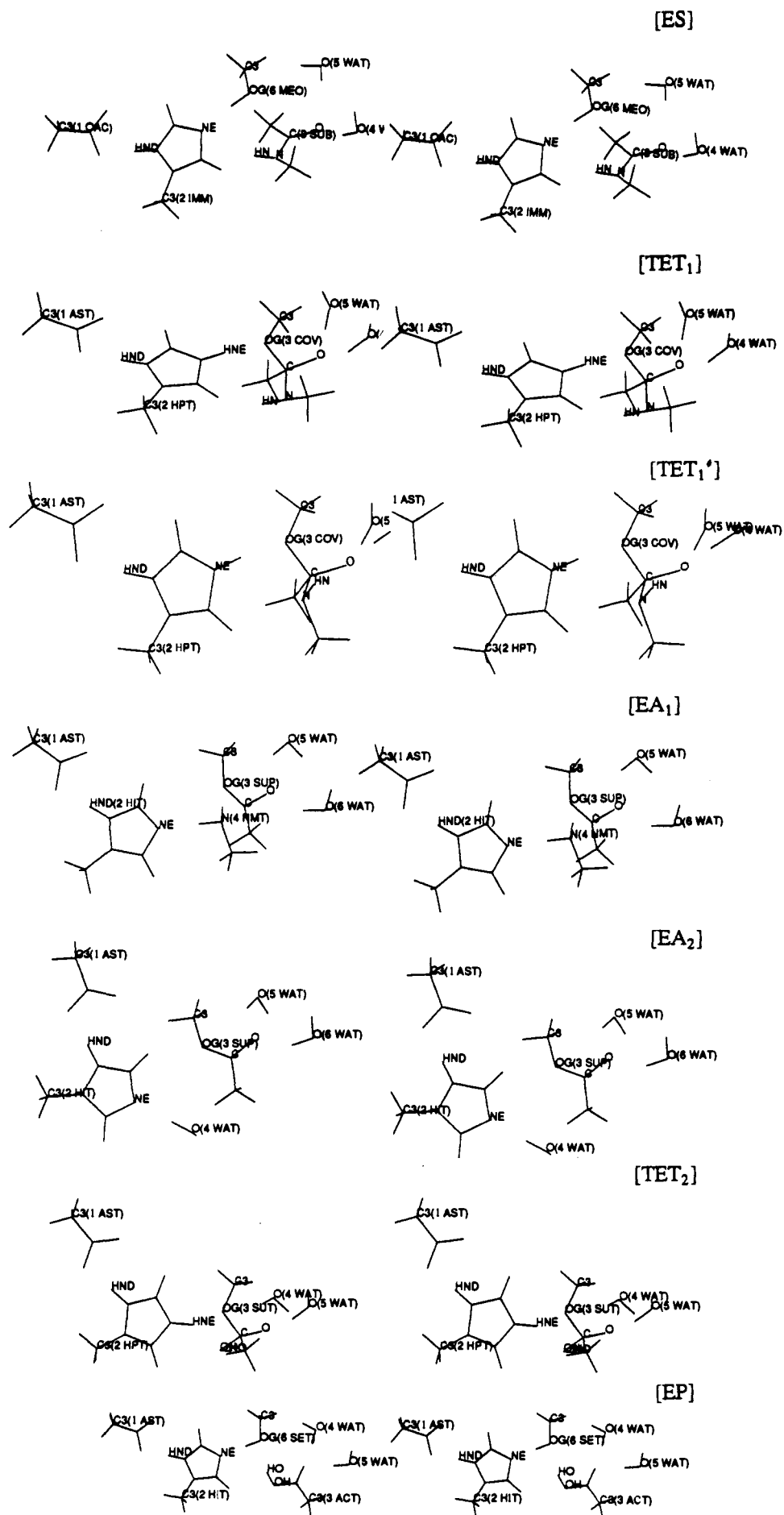


Figure 4. Stereoviews of optimized structures along the reaction pathway.

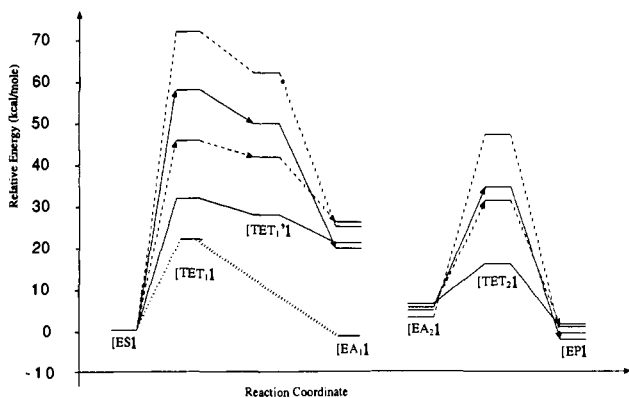


Figure 5. Relative energies of structures along the reaction path as a function of environment. Within each curve, the energies are relative to the energy of the appropriate starting structure. The solid line is for the full system as shown in Figure 3; the solid line with an arrow is for the system without the Asp mimic; the dashed line with an arrow is for the system without the waters representing the oxyanion hole; the dashed line is for the system without Asp and without the oxyanion hole; and the final line extending only as far as [EA] is with the ester substrate. The energies for the starting structures were -357.81 kcal/mol with all the molecules as shown in Figures 3 and 4; -200.76 kcal/mol without the Asp; -239.13 kcal/mol without the two water molecules; -84.88 kcal/mol without the Asp and waters; and -396.19 kcal/mol for the ester complex.

reaction pathway studies described here. PM3 produced much better hydrogen bond geometries than AM1. A major problem with using AM1 to study serine protease catalysis is that the complex between the positively charged histidine mimic and acetate (for Asp) was not stable (i.e., not even a local minimum). Instead of maintaining their charged states, the acetate molecule abstracted one of the imidazole's protons. Protonated Asp is not observed experimentally.^{10,11} Hence, PM3 was the better molecular model for this system where hydrogen bonding is clearly important and where the process of interest is occurring in the enzyme active site as opposed to the gas phase. Nonetheless, when the proton was forced to transfer from His to Asp with PM3, a lower energy was found for the double-proton-transfer structure than the triple ion by ~ 15 kcal/mol. This may be real or an artifact of PM3. Until definitive ab initio calculations are done, one does not know whether isolated $\text{Asp}^-\text{His}^+\text{Ser}^-$ or $\text{Asp}^0\text{His}^0\text{Ser}^-$ is more stable in vacuo. But, in our opinion, the overall environmental effects as well as specific hydrogen bonding to Asp 102 will cause $\text{Asp}^-\text{His}^+\text{Ser}^-$ to be more stable in the active site of trypsin.^{10,11} The fact that PM3 at least has a local minimum for this structure (and AM1 does not) allows us to study what we consider to be the relevant mechanism. The discussion that follows focuses on the reaction pathway studies unless the molecular mechanics or dynamics results are mentioned specifically.

Overall Comparison to Experiment. For the reaction pathway for serine proteases shown in Figure 3, the rate-limiting step was formation of the first tetrahedral intermediate with both of the substrates. The calculated activation energy for this process was 31 kcal/mol for the amide substrate. This value is in the ballpark of the experimental activation energy of approximately 20 kcal/mol for various amide substrates (the experimental value was estimated from the experimental rate constants¹ using transition-state theory). Our calculated activation energy is high, though, for a couple of reasons: We computed potential energy differences while the experimental value is an activation free energy, and we used a reduced representation of the active site. As pointed out by a reviewer, by considering the pK_a difference between the Ser and His, the energy for proton transfer would be expected to be roughly 10 kcal/mol in water (12 kcal/mol with some degree of electrostatic stabilization that is estimated to yield roughly 10 kcal/mol). However, we are not sure what the value should be in the protein interior. Therefore, instead of attempting to correct our in vacuo energies in an ad hoc manner, because there is no way to rigorously do so, we prefer to simply present our results, but one must keep in mind that the model is very simplistic

and may affect the conclusions drawn. Experimentally, the rate-limiting step for amide hydrolysis is acylation and is deacylation for ester hydrolysis.¹ And, on the basis of pre-steady-state kinetic studies, formation of the tetrahedral intermediate preceding the breakdown to the acylenzyme appears to be the actual rate-determining step for amides.^{31,32} We did not observe differences in the rate-limiting step with the different substrates although the activation energy for acylation was lower with the ester than the amide. If arguments regarding motion are invoked, deacylation becomes the rate-determining step with the ester, though (discussed below).

Mechanism of Acylation. Although many investigators have examined the mechanism of formation of the tetrahedral intermediate, the question has not been definitively resolved. After the catalytic triad was first observed,³³ it was suggested that the nucleophilicity of the serine was increased by a concerted transfer of two protons, $\text{Ser} \rightarrow \text{His} \rightarrow \text{Asp}$.³⁴ Although this mechanism was generally accepted for a number of years, more recent NMR^{11,35} and neutron diffraction studies¹⁰ indicate that the triple ion ($\text{Asp}^-\cdots\text{His}^+\cdots\text{Ser}^-$) is favored over the double-proton-transfer-generated structure ($\text{AspH}^-\cdots\text{His}^-\cdots\text{Ser}^-$) in the tetrahedral intermediate. A recent study using chymotrypsin methylated at N_ϵ of the His, which blocks the double proton transfer, also suggests that Asp will remain ionized.³⁶ These findings suggest, then, that the Asp will remain ionized in the transition state as well,⁴ but a proton transfer at the transition state cannot be ruled out.

Many quantum mechanical calculations employing a system composed entirely of the catalytic triad (or reduced representations of the triad) without the surrounding protein support the concerted double-proton-transfer mechanism.⁶⁻⁸ Studies by Kollman and Hayes using a limited system, however, concluded that the triple ion ($\text{Asp}^-\cdots\text{His}^+\cdots\text{Ser}^-$) is lower in energy than ($\text{AspH}^-\cdots\text{His}^-\cdots\text{Ser}^-$).^{9,37} The key difference between these studies with opposing views of the proton transfer is the inherent proton affinity of various groups; PM3 and AM1 are much better than previous semiempirical models and many ab initio models at representing proton affinities. Calculations including the protein environment have also contradicted the concerted double-proton-transfer mechanism.^{4,38} Calculations presented here on our simple model are also consistent with the single-proton-transfer mechanism; we never observed proton transfer from the histidine to the aspartate (Table I). Nor did we ever observe a bifurcated hydrogen bond to the Asp.

It is probably misleading to speak of triple ions in the reaction pathway of the serine proteases, because it is unlikely that a bare methoxide (MeO^-) is produced. Kollman and Hayes³⁷ found the $\text{Ser} \rightarrow \text{His}$ proton transfer accompanied by Ser attack on the substrate with an upper bound of 27 kcal/mol. Other researchers have found or assumed that proton transfer is approximately complete prior to nucleophilic attack.³⁴ Our work here shows almost the opposite proton-transfer behavior. We found that the lowest energy path for formation of the tetrahedral intermediate was for serine first to approach the substrate. When serine's oxygen was within approximately 2 Å of the substrate carbon, proton transfer began. Finally, from this position, Ser attack and proton transfer occurred simultaneously. This mechanism involving coupled heavy atom movement and proton transfer suggests

(31) Hirohara, H.; Bender, M. L.; Stark, R. S. *Proc. Natl. Acad. Sci. U.S.A.* **1974**, *71*, 1643-1647.

(32) Hirohara, H.; Philipp, M.; Bender, M. L. *Biochemistry* **1977**, *16*, 1573-1580.

(33) Blow, D. M.; Birktoft, J. J.; Hartley, B. S. *Nature* **1969**, *221*, 337-340.

(34) Hunkapiller, M. W.; Smallcombe, S. H.; Whitaker, D. R.; Richards, J. H. *Biochemistry* **1973**, *12*, 4732-4743.

(35) Bachovchin, W. W.; Roberts, J. D. *J. Am. Chem. Soc.* **1978**, *100*, 8041-8047.

(36) Sholten, J. D.; Hogg, J. L.; Raushel, F. M. *J. Am. Chem. Soc.* **1988**, *110*, 8246-8247.

(37) Kollman, P. A.; Hayes, D. M. *J. Am. Chem. Soc.* **1981**, *103*, 2955-2961.

(38) Umeyama, H.; Nakagawa, S.; Kudo, T. *J. Mol. Biol.* **1981**, *150*, 409.

that there is protonic bridging in the transition state, which is consistent with isotope-effect experiments.^{5,39}

Our estimate of the activation barrier is probably an upper bound for the formation of the tetrahedral intermediate, as dynamical fluctuations bringing O_γ and the carbonyl carbon of the substrate near in space will facilitate catalysis. A fluctuation bringing O_γ of the serine within 2.1 Å of the carbonyl carbon could decrease the activation energy of amide hydrolysis to 18 kcal/mol (Table II), and the activation energy for the hydrolysis of the ester would decrease to 9 kcal/mol (Table III). If this same argument is applied to the deacylation step, thermal motion bringing the water closer to the acylated serine would lower the activation energy for this process to 12 kcal/mol. A fluctuation of this magnitude (~ 1.2 Å) is possible although probably relatively rare, like catalysis itself. In any case, if thermal motion facilitates heavy atom motion, acylation would still have the higher activation barrier with amides but the barrier to deacylation would be greater than for acylation with esters. Then, the final step, that of $TET_2 \rightarrow EP$, would be rate limiting for the ester with an activation barrier of 14.2 kcal/mol. If we again attempt to account for motion and in this case assume that protein motion could bring the proton on the histidine 0.4 Å closer to O_γ of the serine, the reaction occurs without an activation barrier. Thus, allowing that the motion can be facilitated in this way, these results are consistent with the experimental findings. In our molecular dynamics simulation, the minimum O_γ -C distance that we observed was 2.5 Å, not 2.1 Å. Thus, we did see thermally induced motion that brought O_γ near the carbonyl carbon. That we did not observe shorter distances is due partly to the relatively short simulation time and mostly due to the steep repulsive term in the molecular mechanical potential function that keeps atoms from getting too close. Hence, this mechanism for decreasing the barrier to activation still seems reasonable, but it may require the use of other methods (for example, coupled quantum mechanics and molecular dynamics) or altered simulation techniques for verification because of the inherent problem with the simulation of rare events and the nonbonded energy term used.

Komiyama and Bender have proposed another model for serine protease catalysis.⁴⁰ They suggest that a tetrahedral intermediate is not formed at all. Instead, they propose that a proton is donated directly to the nitrogen without ever forming the C-O bond between serine and the substrate. There is experimental evidence that inhibitors with tetrahedral geometry bind more tightly than substrates, which albeit circumstantial, is in opposition to Komiyama and Bender's proposal. Also, there is an entropic advantage to use only one proton transfer rather than to engineer precise alignment of all three residues for concerted proton transfer.⁴¹

Schowen and co-workers have found that for normal substrates only one proton transfer is indicated in the transition state using solvent isotope effects and the proton inventory technique.^{42,43} Further, they show that two protons appear to be transferred with very good substrates, suggesting the importance of interactions between the substrate and the enzyme at sites distant from the active site. The first proton transfer is attributed to the Ser \rightarrow His movement, as mentioned above. The second transferred proton has been attributed to His \rightarrow Asp; however, on the basis of all the experimental and theoretical evidence, this is unlikely. Alternatively, "compressive forces" leading to a bridging hydrogen between His and Asp have been proposed to be responsible.⁵ Other possible reasons are the formation or strengthening of a number of hydrogen bonds in the tetrahedral intermediate⁴⁴ or that better

hydrogen bonds are formed with the oxyanion hole in the tetrahedral intermediate than in the Michaelis complex. Our results support this last hypothesis. In our calculations, the hydrogen bonds to the oxyanion improved greatly in forming the tetrahedral intermediate (1.81 \rightarrow 1.77 Å and 2.53 \rightarrow 1.75 Å). The hydrogen bonds to Asp only improved slightly (<0.1 Å), which is in opposition to the hypothesis regarding "compression" of the Asp and His.⁵ We did not observe substantial differences in other hydrogen bonds. Hence, our results suggest that the improved hydrogen bonds to the oxyanion may be responsible for the apparent second proton transfer in good substrates. But, given our reduced system, the other alternatives cannot be ruled out.

The theory of stereoelectronic control has also been applied to the acylation pathway of serine proteases.^{45,46} Molecular orbital calculations provide support for Deslongchamps' work⁴⁷ demonstrating selective cleavage of bonds that are trans-antiperiplanar (app) to lone pairs on directly bonded oxygen or nitrogen atoms on compounds with tetrahedral carbons.⁴⁸ The stereoelectronic effect is presumed to be due to interactions between a σ^* antibonding C-X₁ orbital with the app lone pair on X₂, where X = oxygen or nitrogen.⁴⁹ Or, in other words, this effect has a double bond-no bond resonance contribution, thereby making the particular bond easier to make or break.⁴⁶ Furthermore, Gorenstein and co-workers suggest that the stereoelectronic effect is more important in the transition states than in the ground states or intermediates.⁴⁹

For our purposes, the application of this theory, as presented by Taira and Gorenstein,⁴⁶ to serine proteases stresses two factors for amide hydrolysis: that C-O bond rotation of the serine occurs and that the nitrogen of the substrate is inverted after formation of the tetrahedral intermediate. For nucleophilic attack by the serine, the most stereoelectronically favored transition state possesses a nitrogen lone pair app to the nascent O-C bond while not containing a lone pair on the serine oxygen that is app to the substrate's N-C bond. Then, to facilitate N-C cleavage, the lone pair on the serine oxygen must be app to the scissile bond and the nitrogen should not have a lone pair app to the serine substrate bond. This conformation is achieved by N-inversion and a conformational change in the serine, causing kinking of the C_β - O_γ -C angle. The N-inversion stabilizes the intermediate by 3.1 kcal/mol.⁴⁶ It has also been argued that the nitrogen inversion prevents reversion to the Michaelis complex, thus acting as a switch controlling whether the C-O bond or the C-N bond is broken.⁴⁵ These stereoelectronic arguments have recently been invoked to construct models of the tetrahedral intermediate in the active site of trypsin and to investigate the resulting structural changes in the protein.⁵⁰

In our calculations, we found kinking of the serine side chain as proposed by Taira and Gorenstein; however, we observed the conformational change in the serine during the formation of the first tetrahedral intermediate, and the resulting conformation was maintained in the N-inverted form of the intermediate. But, the lone pairs, as required by the stereoelectronic effect, may have been altered with rotation of the nitrogen while θ_1 of Table I was maintained. We found that rotation about the nitrogen stabilized the tetrahedral intermediate by 3.9 kcal/mol, which is close to the value reported by Taira and Gorenstein.⁴⁶ This rotation put the nitrogen in a much better position to abstract a proton from the histidine mimic. Our studies cannot distinguish between stereoelectronic control in determining the relative energies of the two forms of the first tetrahedral intermediate (structures TET_1 and TET_1' of Figure 4) and the importance of other interactions. The improvement we saw in rotating about the nitrogen could be

(39) Satterthwait, A. C.; Jencks, W. P. *J. Am. Chem. Soc.* **1974**, *96*, 7018.

(40) Komiyama, M.; Bender, M. *Proc. Natl. Acad. Sci. U.S.A.* **1979**, *76*, 557-560.

(41) Scheiner, S.; Hillebrand, E. *Proc. Natl. Acad. Sci. U.S.A.* **1985**, *82*, 2741-2745.

(42) Stein, R. L.; Elrod, J. P.; Schowen, R. L. *J. Am. Chem. Soc.* **1983**, *105*, 2446-2452.

(43) Elrod, J. P.; Hogg, J. L.; Quinn, D. M.; Venkatasubban, K. S.; Schowen, R. L. *J. Am. Chem. Soc.* **1980**, *102*, 3917-3922.

(44) Fink, A. In *Enzyme Mechanisms*; Page, M. J., Williams, A., Eds.; Royal Society of Chemistry: London, 1987; p 159.

(45) Bizzozero, S. A.; Dutler, H. *Bioorg. Chem.* **1981**, *10*, 46-62.

(46) Taira, K.; Gorenstein, D. G. *Bull. Chem. Soc. Jpn.* **1987**, *60*, 3625-3632.

(47) Deslongchamps, P. *Stereoelectronic Effects in Organic Chemistry*; Pergamon Press: Oxford, 1983.

(48) Gorenstein, D. G.; Taira, K. *Biophys. J.* **1984**, *46*, 749.

(49) Gorenstein, D. G.; Luxon, B. A.; Goldfield, E. M. *J. Am. Chem. Soc.* **1980**, *102*, 1757.

(50) Dutler, H.; Bizzozero, S. A. *Acc. Chem. Res.* **1989**, *22*, 322-327.

due to release of H-H repulsion with nitrogen inversion that leads to favorable N...H interactions. It has been pointed out by Asboth and Polgar that hydrogen bonding, or any other significant interaction with the protein environment, could override stereo-electronic control.⁵¹ There are also a number of other problems with stereoelectronic theory as applied to serine proteases, and they have been reviewed by Fink.⁴⁴

Mechanism of Deacylation. In the case of the deacylation step (formation of the second tetrahedral intermediate), we also found that the low-energy path was for approach of the water, partial transfer of the proton, and then simultaneous attack and transfer (Table IV). Concerted proton transfer and attack had the same activation energy, although it was not the low-energy path considering the individual steps. On the basis of our results, if the enzyme had to deprotonate the water completely, prior to attack, this step would have the rate-determining activation barrier. By allowing attack to occur with deprotonation, the activation barrier was lowered by approximately 24 kcal/mol. Warshel and co-workers⁵² have also pointed out how enzymes cannot use bare water molecules because of the high energy required to strip off a proton (~22 kcal/mol) and how metals and protein residues can aid in this process to lower the barrier.

Importance of Enzyme Conformation on Catalysis. So far we have only discussed proton transfer and nucleophilic attack without considering the importance of conformation. Enzymes act by lowering the activation free energies of the reactions they catalyze. This can be accomplished in a variety of ways: (1) active sites with electrostatic complementarity to the transition state, (2) inducing strain in the substrate, and (3) with substrate binding that induces a change in the enzyme such that it becomes more reactive. Warshel and co-workers have argued persuasively for the importance of the first mechanism for serine proteases,^{4,52} and our molecular mechanical energy decomposition of important interactions in the covalent versus the noncovalent complex further supports this idea; this possibility is discussed further below. The second mechanism had gained support from the fact that the binding site is complementary to the structure of the tetrahedral intermediate.^{53,54} There is NMR evidence, however, that the carbonyl carbon of the substrate remains relatively planar in the Michaelis complex and hence that there is little to no distortion of the substrate on binding.^{55,56} In our models, the carbon did indeed remain planar in the presence of the active site residues and was not induced to adopt the tetrahedral geometry. On work with transition-state analogues it has been suggested that the major driving force for catalysis is the distortion of the scissile bond from planarity by the enzyme, thereby eliminating the stabilization energy of the peptide bond.⁵⁷ In our models, we found comparable values for the ω dihedral angle in the substrate, in the substrate complex with water molecules, and in the structure with the active site residues ($\omega = 161, 163, \text{ and } 155^\circ$, respectively). Thus, our results are inconsistent with this hypothesis, but given our limited representation of the active site, we cannot rule out the strain hypotheses. Warshel and co-workers have pointed out that even a change in geometry of the carbonyl carbon from sp^2 to sp^3 results in less than a 0.3-Å displacement of the surrounding atoms, which can easily be accommodated by the flexible enzyme.⁵²

The third possible manner for lowering the activation energy of a process is for the substrate to induce a change in the enzyme that favors catalysis. This appeared to be the case with serine proteases. For many years, it was thought that the Ser and His of the catalytic triad did not form a hydrogen bond in the Mi-

chaelis complex.⁵⁸ It has been shown more recently that a hydrogen bond is present in most free serine proteases.^{12,59} These residues also form a strong hydrogen bond in the presence of substrate.⁶⁰ In the molecular dynamics simulation, this hydrogen bond was broken approximately 25% of the time. It may be that this interaction is involved in control of catalysis by ensuring the enzyme is not always "on". Instead, this mechanism for lowering the activation energy may be due merely to burying of the charge relay system when substrate or inhibitor is bound, enhancing the polarizing influence of the system.⁵ In our simple system, we observed a slightly long but acceptable hydrogen bond between the Ser and His mimics in the model complex (2.49 Å) that decreased in the presence of the substrate (1.76 Å).

Effect of Environment on Catalysis. What is the role of environmental effects on the catalytic process? Asp and the oxyanion hole are critical components of the active site and, in fact, have been seen in all serine proteases to date.² One of the hydrogen bonds to the oxyanion hole is long in the Michaelis complex.¹ But strong hydrogen bonds are formed with each as the reaction proceeds from $C=O \rightarrow C-O^-$.⁶¹ The oxyanion hole forms strong hydrogen bonds with the oxyanion of transition-state analogue inhibitors.^{10,11} Thus, the oxyanion hole appears to not only be suited for binding the transition state or tetrahedral intermediate but to stabilize the developing negative charge on the oxygen. We also found a long hydrogen bond initially in our models that decreased as the tetrahedral intermediate was formed (Table I). Removing the oxyanion hole waters from our models for amide hydrolysis had a drastic effect on the stability of the tetrahedral intermediates, destabilizing them by 13–14 kcal/mol. We also observed the importance of the oxyanion hole in the molecular mechanical calculations with the enzyme fully present. This can be related to the lower enzymatic activity (10^{-4} – 10^{-7}) of serine protease zymogens compared to that of active enzymes.¹² The major difference in the zymogens appears to be the lack of the oxyanion hole.

Aspartate may be an invariant member of the active site of serine proteases because of its role in stabilizing the transition state through electrostatic interactions.^{4,52,62} This is important because the formation of the transition state involves a drastic change in the charge distribution, which is akin to the formation of an ion pair from a neutral ground state.⁵² Another possibility is that the Asp is there to raise the pK_a of the histidine and confine its location.^{63,64} All of these mechanisms are probably in effect.

We found that the Asp mimic in our models for amide hydrolysis stabilized the first tetrahedral intermediate system and its N-inverted form by 27 and 22 kcal/mol, respectively. Asp was destabilizing for the other intermediate states (besides the second tetrahedral intermediate); the largest effect was on the enzyme-product complex. The destabilizing effect of the Asp in this case may be to keep the enzyme-product complex from being too stable so that the enzyme can be regenerated for further hydrolysis reactions. We found that the oxyanion hole hydrogen bonds stabilized the tetrahedral systems by approximately 14 kcal/mol. Overall, we found the Asp to be more important in stabilizing the tetrahedral intermediates, and therefore presumably the transition states, than the oxyanion hole. The stability afforded these states by the Asp is due almost entirely to interactions with the His (data not presented). Our values for the stabilization provided by the Asp and oxyanion hole are exaggerated, however, compared to experiment because of the limited representation of the environment. More sophisticated calculations may be necessary to obtain quantitative agreement with experiment such as those presented by Russell and Warshel.⁵² Experimentally, the replacement of

(51) Asboth, B.; Polgar, L. *Biochemistry* **1983**, *22*, 117–122.

(52) Warshel, A.; Naray-Szabo, G.; Sussman, F.; Hwang, J. K. *Biochemistry* **1989**, *28*, 3629–3637.

(53) Henderson, R.; Wright, C. S.; Hess, G. P.; Blow, D. M. *Cold Spring Harbor Symp. Quant. Biol.* **1971**, *36*, 63–70.

(54) Poulos, T. L.; Alden, R. A.; Freer, S. T.; Birktoft, J. J.; Kraut, J. J. *Biol. Chem.* **1976**, *251*, 1097–1103.

(55) Baillurgeon, M. W.; Laskowski, M., Jr.; Neves, D. E.; Porubcan, M. A.; Santini, R. E.; Markley, J. L. *Biochemistry* **1980**, *19*, 5703–5710.

(56) Richarz, R.; Tschesche, H.; Wuthrich, K. *Biochemistry* **1980**, *19*, 5711–5715.

(57) Delbaere, L. T. J.; Brayer, G. D. *J. Mol. Biol.* **1985**, *183*, 39–103.

(58) Brayer, G. D.; Delbaere, L. T. J.; James, M. N. G. *J. Mol. Biol.* **1979**, *131*, 743.

(59) Tsukada, H.; Blow, D. M. *J. Mol. Biol.* **1985**, *184*, 703.

(60) Huber, R.; Bode, W. *Acc. Chem. Res.* **1978**, *11*, 114.

(61) Fersht, A. R.; Blow, D. M.; Fastrez, J. *Biochemistry* **1973**, *12*, 2035.

(62) Nakagawa, S.; Umeiyama, H. *J. Mol. Biol.* **1984**, *179*, 103–123.

(63) Fersht, A. R.; Sperling, J. J. *J. Mol. Biol.* **1978**, *74*, 137.

(64) Sprang, S.; Standing, T.; Fletterick, R. J.; Stroud, R. M.; Finer-Moore, J.; Xuong, N.-H.; Hamlin, R.; Rutter, W. J.; Craik, C. S. *Science* **1987**, *238*, 905.

Asp by a neutral residue destabilizes the transition state by approximately 4–6 kcal/mol.⁶⁵ Experimentally, one hydrogen bond of the oxyanion hole contributes about 5 kcal/mol to stabilization of the tetrahedral intermediate.⁶⁶

Summary

We present both semiempirical molecular orbital and molecular mechanical calculations to study the serine protease catalyzed hydrolysis of amides and esters and the effect of the protein environment and dynamics on this process. The lowest energy pathway for formation of the tetrahedral intermediate was for serine to approach the substrate, followed by coupled heavy atom movement and protein transfer to complete the reaction. The reaction pathway calculations were performed with a truncated active site model. We do not mean to suggest with the use of such a reduced representation of the serine protease active site that the protein is unimportant in catalysis, especially in light of evidence indicating that specific side chain interactions between substrate and enzyme sites remote from the active site can alter both the rate of catalysis and the mechanism.⁵ Due to system

size limitations, though, one is forced to employ truncated systems even with semiempirical methods. It is interesting, though, that the environment itself, excluding the key active site residues and interactions, was important in stabilizing the substrate and did so better in the covalent than noncovalent complex. Hence, other residues besides those that we included in the semiempirical calculations are important, but we find it gratifying that such a simple model can reproduce many aspects of serine protease catalysis. Inclusion of the protein environment and surrounding solvent in a more sophisticated way will, no doubt, be necessary for quantitative agreement with experiment, but we find these initial results encouraging and informative. Our studies suggest modes of proton transfer and nucleophilic attack that are consistent with the experimental results and, to our knowledge, novel. In the future, we hope to pursue studies combining both quantum mechanics and molecular dynamics directly to more fully account for environmental effects.

Acknowledgment. We are grateful for research support from the NIH (Grant GM-29072), the NSF (Grant DMB-87-14775), and DARPA (Grant N00014-86-K-0757). S.S. thanks the Deutsche Forschungsgemeinschaft for a postdoctoral fellowship.

Registry No. His, 71-00-1; Asp, 56-84-8; Ser, 56-45-1; Gly, 56-40-6; trypsin, 9002-07-7; serine proteinase, 37259-58-8.

(65) Craik, C. S.; Rozniak, S.; Largeman, C.; Rutter, W. J. *Science* **1987**, *237*, 909.

(66) Wells, J. A.; Cunningham, B. C.; Graycar, T. P.; Estell, D. A. *Philos. Trans. R. Soc. London* **1986**, *A317*, 415.

Roles of Zinc(II) Ion in Phosphatases. A Model Study with Zinc(II)–Macrocyclic Polyamine Complexes

Tohru Koike[†] and Eiichi Kimura^{*†,‡}

Contribution from the Department of Medicinal Chemistry, Hiroshima University School of Medicine, Kasumi 1-2-3, Minami-ku, Hiroshima 734, Japan, and Coordination Chemistry Laboratories, Institute for Molecular Science, Nishigo-naka, 38, Myodaiji, Okazaki 444, Japan. Received April 12, 1991

Abstract: The zinc(II) complexes of 1,5,9-triazacyclododecane (L_4 , [12]aneN₃) and 1,4,7,10-tetraazacyclododecane (L_2 , [12]aneN₄) promote the hydrolysis of tris(4-nitrophenyl) phosphate, TNP^0 (a neutral phosphotriester), and bis(4-nitrophenyl) phosphate, BNP^- (a monoanionic phosphodiester). Kinetic studies show that the reactive species are commonly $L-Zn^{II}-OH^-$ and the kinetically obtained pK_a values are almost identical to those obtained thermodynamically ($pK_a(H_2O)$). The comparative reactivities of OH^- , $L_4-Zn^{II}-OH^-$, and $L_2-Zn^{II}-OH^-$ with different $pK_a(H_2O)$ values of 15.7, 7.3, and 8.0 have been studied to understand the role of Zn^{II} in alkaline phosphatases. For the neutral phosphotriester TNP^0 , the second-order rate constants ($M^{-1} s^{-1}$) at 25 °C and $I = 0.20$ are 10.7, 7.0, and 3.7, respectively, indicating free OH^- ion (the most basic OH^- species) is the best promoter. On the other hand, toward the anionic phosphodiester BNP^- , the $L_4-Zn^{II}-OH^-$ becomes more efficient than free OH^- ion: The second-order rate constants ($\times 10^5, M^{-1} s^{-1}$) are 2.4, 8.5, and 2.1, respectively, at 35 °C and $I = 0.20$. A bifunctional ("hybrid") mechanism of Zn^{II} (especially the $Zn^{II}-L_4$ system) toward phosphates (especially the anionic phosphate), in which the Zn^{II} -bound OH^- acts as a nucleophile, while the vacant Zn^{II} coordination site anchors the substrate $P=O$ or $P-O^-$ group, is well disclosed by comparing these kinetic results with the second-order rate constants (at 25 °C and $I = 0.10$) of 4-nitrophenyl acetate hydrolysis, $9.5, 4.1 \times 10^{-2}$, and $1.1 \times 10^{-1} M^{-1} s^{-1}$, respectively, where all of the OH^- species act merely as nucleophiles to the carbonyl group, as indicated by a linear relationship between the $pK_a(H_2O)$ values and the rate constants. Phosphate anion affinity constants $K(A^-)$ (M^{-1}) with the $Zn^{II}-L_4$ complex determined by pH titration are $10^{3.5}$ for phenyl phosphate, PP^{2-} , and $10^{3.1}$ for 4-nitrophenyl phosphate, NP^{2-} , which are ca. 25 times larger than those with the less acidic Zn^{II}_{aq} ion.

Introduction

Zinc(II) ion plays a vital role in Zn^{II} -containing phosphate esterases.¹ Although there have been numerous reports of the esterase model systems² using well-defined metal (e.g., Co^{III} ,³ Cu^{II} ,^{4,5} Ni^{II} ,⁵ Zn^{II} ,^{5,6a} La^{III} ,^{6b} and Ir^{III})⁷ complexes, most were addressed to attaining better acceleration of the hydrolysis rates

and their applications. Only a few Zn^{II} model complexes^{8,9} were studied on the reactivities in hydrolysis of neutral phosphotriesters.

(1) (a) Coleman, J. E. In *Zinc Enzymes*; Birkhäuser: Boston, MA, 1986; Chapter 4, p 49. (b) Coleman, J. E.; Gettins, P. Ibid; Chapter 6, p 77. (c) Coleman, J. E.; Gettins, P. *Adv. Enzymol.* **1983**, *55*, 381.

(2) Recent review articles: (a) Basile, L. A.; Barton, J. K. *Met. Ions Biol. Syst.* **1989**, *25*, 31. (b) Sigel, H. *Coord. Chem. Rev.* **1990**, *100*, 453. (c) Breslow, R. *Adv. Enzymol.* **1986**, *58*, 1.

[†]Hiroshima University School of Medicine.

[‡]Institute for Molecular Science.